

Production of Z^0 bosons in elastic and quasi-elastic ep collisions at HERA

ZEUS Collaboration

Abstract

The production of Z^0 bosons in the reaction $ep \rightarrow eZ^0p^{(*)}$, where $p^{(*)}$ stands for a proton or a low-mass nucleon resonance, has been studied in ep collisions at HERA using the ZEUS detector. The analysis is based on a data sample collected between 1996 and 2007, amounting to 496 pb^{-1} of integrated luminosity. The Z^0 was measured in the hadronic decay mode. The elasticity of the events was ensured by a cut on $\eta_{\text{max}} < 3.0$, where η_{max} is the maximum pseudorapidity of energy deposits in the calorimeter defined with respect to the proton beam direction. A signal was observed at the Z^0 mass. The cross section of the reaction $ep \rightarrow eZ^0p^{(*)}$ was measured to be $\sigma(ep \rightarrow eZ^0p^{(*)}) = 0.13 \pm 0.06 \text{ (stat.)} \pm 0.01 \text{ (syst.) pb}$, in agreement with the Standard Model prediction of 0.16 pb . This is the first measurement of Z^0 production in ep collisions.

The ZEUS Collaboration

H. Abramowicz^{45,ah}, I. Abt³⁵, L. Adamczyk¹³, M. Adamus⁵⁴, R. Aggarwal^{7,c}, S. Antonelli⁴, P. Antonioli³, A. Antonov³³, M. Arneodo⁵⁰, O. Arslan⁵, V. Aushev^{26,27,aa}, Y. Aushev^{27,aa,ab}, O. Bachynska¹⁵, A. Bamberger¹⁹, A.N. Barakbaev²⁵, G. Barbagli¹⁷, G. Bari³, F. Barreiro³⁰, N. Bartosik¹⁵, D. Bartsch⁵, M. Basile⁴, O. Behnke¹⁵, J. Behr¹⁵, U. Behrens¹⁵, L. Bellagamba³, A. Bertolin³⁹, S. Bhadra⁵⁷, M. Bindi⁴, C. Blohm¹⁵, V. Bokhonov^{26,aa}, T. Bold¹³, K. Bondarenko²⁷, E.G. Boos²⁵, K. Borras¹⁵, D. Boscherini³, D. Bot¹⁵, I. Brock⁵, E. Brownson⁵⁶, R. Brugnera⁴⁰, N. Brümmer³⁷, A. Bruni³, G. Bruni³, B. Brzozowska⁵³, P.J. Bussey²⁰, B. Bylsma³⁷, A. Caldwell³⁵, M. Capua⁸, R. Carlin⁴⁰, C.D. Catterall⁵⁷, S. Chekanov¹, J. Chwastowski^{12,e}, J. Ciborowski^{53,al}, R. Ciesielski^{15,h}, L. Cifarelli⁴, F. Cindolo³, A. Contin⁴, A.M. Cooper-Sarkar³⁸, N. Coppola^{15,i}, M. Corradi³, F. Corriveau³¹, M. Costa⁴⁹, G. D'Agostini⁴³, F. Dal Corso³⁹, J. del Peso³⁰, R.K. Dementiev³⁴, S. De Pasquale^{4,a}, M. Derrick¹, R.C.E. Devenish³⁸, D. Dobur^{19,u}, B.A. Dolgoshein^{33,†}, G. Dolinska²⁷, A.T. Doyle²⁰, V. Drugakov¹⁶, L.S. Durkin³⁷, S. Dusini³⁹, Y. Eisenberg⁵⁵, P.F. Ermolov^{34,†}, A. Eskreys^{12,†}, S. Fang^{15,j}, S. Fazio⁸, J. Ferrando²⁰, M.I. Ferrero⁴⁹, J. Figiel¹², B. Foster^{38,ad}, G. Gach¹³, A. Galas¹², E. Gallo¹⁷, A. Garfagnini⁴⁰, A. Geiser¹⁵, I. Gialas^{21,x}, A. Gizhko^{27,ac}, L.K. Gladilin³⁴, D. Gladkov³³, C. Glasman³⁰, O. Gogota²⁷, Yu.A. Golubkov³⁴, P. Göttlicher^{15,k}, I. Grabowska-Bold¹³, J. Grebenyuk¹⁵, I. Gregor¹⁵, G. Grigorescu³⁶, G. Grzelak⁵³, O. Gueta⁴⁵, M. Guzik¹³, C. Gwenlan^{38,ae}, T. Haas¹⁵, W. Hain¹⁵, R. Hamatsu⁴⁸, J.C. Hart⁴⁴, H. Hartmann⁵, G. Hartner⁵⁷, E. Hilger⁵, D. Hochman⁵⁵, R. Hori⁴⁷, A. Hüttmann¹⁵, Z.A. Ibrahim¹⁰, Y. Iga⁴², R. Ingber⁴⁵, M. Ishitsuka⁴⁶, H.-P. Jakob⁵, F. Januschek¹⁵, T.W. Jones⁵², M. Jünger⁵, I. Kadenko²⁷, B. Kahle¹⁵, S. Kananov⁴⁵, T. Kanno⁴⁶, U. Karshon⁵⁵, F. Karstens^{19,v}, I.I. Katkov^{15,l}, M. Kaur⁷, P. Kaur^{7,c}, A. Keramidis³⁶, L.A. Khein³⁴, J.Y. Kim⁹, D. Kisielewska¹³, S. Kitamura^{48,aj}, R. Klanner²², U. Klein^{15,m}, E. Koffeman³⁶, N. Kondrashova^{27,ac}, O. Kononenko²⁷, P. Kooijman³⁶, Ie. Korol²⁷, I.A. Korzhavina³⁴, A. Kotański^{14,f}, U. Kötz¹⁵, H. Kowalski¹⁵, O. Kuprash¹⁵, M. Kuze⁴⁶, A. Lee³⁷, B.B. Levchenko³⁴, A. Levy⁴⁵, V. Libov¹⁵, S. Limentani⁴⁰, T.Y. Ling³⁷, M. Lisovyi¹⁵, E. Lobodzinska¹⁵, W. Lohmann¹⁶, B. Lühr¹⁵, E. Lohrmann²², K.R. Long²³, A. Longhin^{39,af}, D. Lontkovskiy¹⁵, O.Yu. Lukina³⁴, J. Maeda^{46,ai}, S. Magill¹, I. Makarenko¹⁵, J. Malka¹⁵, R. Mankel¹⁵, A. Margotti³, G. Marini⁴³, J.F. Martin⁵¹, A. Mastroberardino⁸, M.C.K. Mattingly², I.-A. Melzer-Pellmann¹⁵, S. Mergelmeyer⁵, S. Miglioranza^{15,n}, F. Mohamad Idris¹⁰, V. Monaco⁴⁹, A. Montanari¹⁵, J.D. Morris^{6,b}, K. Mujkic^{15,o}, B. Musgrave¹, K. Nagano²⁴, T. Namssoo^{15,p}, R. Nania³, A. Nigro⁴³, Y. Ning¹¹, T. Nobe⁴⁶, D. Notz¹⁵, R.J. Nowak⁵³, A.E. Nuncio-Quiroz⁵, B.Y. Oh⁴¹, N. Okazaki⁴⁷, K. Olkiewicz¹², Yu. Onishchuk²⁷, K. Papageorgiu²¹, A. Parenti¹⁵, E. Paul⁵, J.M. Pawlak⁵³, B. Pawlik¹², P. G. Pelfer¹⁸, A. Pellegrino³⁶, W. Perlański^{53,am}, H. Perrey¹⁵, K. Piotrkowski²⁹, P. Pluciński^{54,an}, N.S. Pokrovskiy²⁵, A. Polini³, A.S. Proskuryakov³⁴, M. Przybycień¹³, A. Raval¹⁵, D.D. Reeder⁵⁶, B. Reisert³⁵, Z. Ren¹¹, J. Repond¹, Y.D. Ri^{48,ak}, A. Robertson³⁸, P. Roloff^{15,n}, I. Rubinsky¹⁵, M. Ruspa⁵⁰, R. Sacchi⁴⁹, U. Samson⁵, G. Sartorelli⁴, A.A. Savin⁵⁶, D.H. Saxon²⁰, M. Schioppa⁸, S. Schlenstedt¹⁶, P. Schleper²², W.B. Schmidke³⁵, U. Schneekloth¹⁵, V. Schönberg⁵, T. Schörner-Sadenius¹⁵, J. Schwartz³¹, F. Sciulli¹¹, L.M. Shcheglova³⁴, R. Shehzadi⁵, S. Shimizu^{47,n}, I. Singh^{7,c}, I.O. Skillicorn²⁰, W. Słomiński^{14,g}, W.H. Smith⁵⁶, V. Sola²², A. Solano⁴⁹, D. Son²⁸, V. Sosnovtsev³³, A. Spiridonov^{15,q}, H. Stadie²², L. Stanco³⁹, N. Stefaniuk²⁷, A. Stern⁴⁵, T.P. Stewart⁵¹, A. Stifutkin³³, P. Stopa¹², S. Suchkov³³,

G. Susinno⁸, L. Suszycki¹³, J. Sztuk-Dambietz²², D. Szuba²², J. Szuba^{15,r}, A.D. Tapper²³,
E. Tassi^{8,d}, J. Terrón³⁰, T. Theedt¹⁵, H. Tiecke³⁶, K. Tokushuku^{24,y}, J. Tomaszewska^{15,s}, V. Trusov²⁷,
T. Tsurugai³², M. Turcato²², O. Turkot^{27,ac}, T. Tymieniecka^{54,ao}, M. Vázquez^{36,n}, A. Verbytskyi¹⁵,
O. Viazlo²⁷, N.N. Vlasov^{19,w}, R. Walczak³⁸, W.A.T. Wan Abdullah¹⁰, J.J. Whitmore^{41,ag},
K. Wichmann^{15,t}, L. Wiggers³⁶, M. Wing⁵², M. Wlasenko⁵, G. Wolf¹⁵, H. Wolfe⁵⁶, K. Wrona¹⁵,
A.G. Yagües-Molina¹⁵, S. Yamada²⁴, Y. Yamazaki^{24,z}, R. Yoshida¹, C. Youngman¹⁵, O. Zabiegailov^{27,ac},
A.F. Żarnecki⁵³, L. Zawiejski¹², O. Zenaiev¹⁵, W. Zeuner^{15,n}, B.O. Zhautykov²⁵, N. Zhmak^{26,aa},
A. Zichichi⁴, Z. Zolkapli¹⁰, D.S. Zotkin³⁴

- 1 *Argonne National Laboratory, Argonne, Illinois 60439-4815, USA*^A
2 *Andrews University, Berrien Springs, Michigan 49104-0380, USA*
3 *INFN Bologna, Bologna, Italy*^B
4 *University and INFN Bologna, Bologna, Italy*^B
5 *Physikalisches Institut der Universität Bonn, Bonn, Germany*^C
6 *H.H. Wills Physics Laboratory, University of Bristol, Bristol, United Kingdom*^D
7 *Panjab University, Department of Physics, Chandigarh, India*
8 *Calabria University, Physics Department and INFN, Cosenza, Italy*^B
9 *Institute for Universe and Elementary Particles, Chonnam National University,*
10 *Kwangju, South Korea*
11 *Jabatan Fizik, Universiti Malaya, 50603 Kuala Lumpur, Malaysia*^E
12 *Nevis Laboratories, Columbia University, Irvington on Hudson, New York 10027,*
13 *USA*^F
14 *The Henryk Niewodniczanski Institute of Nuclear Physics, Polish Academy of*
15 *Sciences, Krakow, Poland*^G
16 *AGH-University of Science and Technology, Faculty of Physics and Applied Com-*
17 *puter Science, Krakow, Poland*^H
18 *Department of Physics, Jagellonian University, Cracow, Poland*
19 *Deutsches Elektronen-Synchrotron DESY, Hamburg, Germany*
20 *Deutsches Elektronen-Synchrotron DESY, Zeuthen, Germany*
21 *INFN Florence, Florence, Italy*^B
22 *University and INFN Florence, Florence, Italy*^B
23 *Fakultät für Physik der Universität Freiburg i.Br., Freiburg i.Br., Germany*
24 *School of Physics and Astronomy, University of Glasgow, Glasgow, United King-*
25 *dom*^D
26 *Department of Engineering in Management and Finance, Univ. of the Aegean,*
27 *Chios, Greece*
28 *Hamburg University, Institute of Experimental Physics, Hamburg, Germany*^I
29 *Imperial College London, High Energy Nuclear Physics Group, London, United*
30 *Kingdom*^D
31 *Institute of Particle and Nuclear Studies, KEK, Tsukuba, Japan*^J
32 *Institute of Physics and Technology of Ministry of Education and Science of Kaza-*
khstan, Almaty, Kazakhstan
33 *Institute for Nuclear Research, National Academy of Sciences, Kyiv, Ukraine*
34 *Department of Nuclear Physics, National Taras Shevchenko University of Kyiv,*
35 *Kyiv, Ukraine*
36 *Kyungpook National University, Center for High Energy Physics, Daegu, South*
37 *Korea*^K
38 *Institut de Physique Nucléaire, Université Catholique de Louvain, Louvain-la-Neuve,*
39 *Belgium*^L
40 *Departamento de Física Teórica, Universidad Autónoma de Madrid, Madrid,*
41 *Spain*^M
42 *Department of Physics, McGill University, Montréal, Québec, Canada H3A 2T8*^N
43 *Meiji Gakuin University, Faculty of General Education, Yokohama, Japan*^J

- 33 *Moscow Engineering Physics Institute, Moscow, Russia*^O
34 *Lomonosov Moscow State University, Skobeltsyn Institute of Nuclear Physics, Mo-*
scow, Russia^P
35 *Max-Planck-Institut für Physik, München, Germany*
36 *NIKHEF and University of Amsterdam, Amsterdam, Netherlands*^Q
37 *Physics Department, Ohio State University, Columbus, Ohio 43210, USA*^A
38 *Department of Physics, University of Oxford, Oxford, United Kingdom*^D
39 *INFN Padova, Padova, Italy*^B
40 *Dipartimento di Fisica dell' Università and INFN, Padova, Italy*^B
41 *Department of Physics, Pennsylvania State University, University Park,*
Pennsylvania 16802, USA^F
42 *Polytechnic University, Tokyo, Japan*^J
43 *Dipartimento di Fisica, Università 'La Sapienza' and INFN, Rome, Italy*^B
44 *Rutherford Appleton Laboratory, Chilton, Didcot, Oxon, United Kingdom*^D
45 *Raymond and Beverly Sackler Faculty of Exact Sciences, School of Physics,*
Tel Aviv University, Tel Aviv, Israel^R
46 *Department of Physics, Tokyo Institute of Technology, Tokyo, Japan*^J
47 *Department of Physics, University of Tokyo, Tokyo, Japan*^J
48 *Tokyo Metropolitan University, Department of Physics, Tokyo, Japan*^J
49 *Università di Torino and INFN, Torino, Italy*^B
50 *Università del Piemonte Orientale, Novara, and INFN, Torino, Italy*^B
51 *Department of Physics, University of Toronto, Toronto, Ontario, Canada M5S*
1A7^N
52 *Physics and Astronomy Department, University College London, London, United*
Kingdom^D
53 *Faculty of Physics, University of Warsaw, Warsaw, Poland*
54 *National Centre for Nuclear Research, Warsaw, Poland*
55 *Department of Particle Physics and Astrophysics, Weizmann Institute, Rehovot,*
Israel
56 *Department of Physics, University of Wisconsin, Madison, Wisconsin 53706, USA*^A
57 *Department of Physics, York University, Ontario, Canada M3J 1P3*^N

- A* supported by the US Department of Energy
- B* supported by the Italian National Institute for Nuclear Physics (INFN)
- C* supported by the German Federal Ministry for Education and Research (BMBF),
under contract No. 05 H09PDF
- D* supported by the Science and Technology Facilities Council, UK
- E* supported by HIR and UMRG grants from Universiti Malaya, and an ERGS grant
from the Malaysian Ministry for Higher Education
- F* supported by the US National Science Foundation. Any opinion, findings and con-
clusions or recommendations expressed in this material are those of the authors and
do not necessarily reflect the views of the National Science Foundation.
- G* supported by the Polish Ministry of Science and Higher Education as a scientific
project No. DPN/N188/DESY/2009
- H* supported by the Polish Ministry of Science and Higher Education and its grants
for Scientific Research
- I* supported by the German Federal Ministry for Education and Research (BMBF),
under contract No. 05h09GUF, and the SFB 676 of the Deutsche Forschungsge-
meinschaft (DFG)
- J* supported by the Japanese Ministry of Education, Culture, Sports, Science and
Technology (MEXT) and its grants for Scientific Research
- K* supported by the Korean Ministry of Education and Korea Science and Engineering
Foundation
- L* supported by FNRS and its associated funds (IISN and FRIA) and by an Inter-
University Attraction Poles Programme subsidised by the Belgian Federal Science
Policy Office
- M* supported by the Spanish Ministry of Education and Science through funds provided
by CICYT
- N* supported by the Natural Sciences and Engineering Research Council of Canada
(NSERC)
- O* partially supported by the German Federal Ministry for Education and Research
(BMBF)
- P* supported by RF Presidential grant N 3920.2012.2 for the Leading Scientific Schools
and by the Russian Ministry of Education and Science through its grant for Scientific
Research on High Energy Physics
- Q* supported by the Netherlands Foundation for Research on Matter (FOM)
- R* supported by the Israel Science Foundation

- a* now at University of Salerno, Italy
- b* now at Queen Mary University of London, United Kingdom
- c* also funded by Max Planck Institute for Physics, Munich, Germany
- d* also Senior Alexander von Humboldt Research Fellow at Hamburg University, Institute of Experimental Physics, Hamburg, Germany
- e* also at Cracow University of Technology, Faculty of Physics, Mathematics and Applied Computer Science, Poland
- f* supported by the research grant No. 1 P03B 04529 (2005-2008)
- g* supported by the Polish National Science Centre, project No. DEC-2011/01/BST2/03643
- h* now at Rockefeller University, New York, NY 10065, USA
- i* now at DESY group FS-CFEL-1
- j* now at Institute of High Energy Physics, Beijing, China
- k* now at DESY group FEB, Hamburg, Germany
- l* also at Moscow State University, Russia
- m* now at University of Liverpool, United Kingdom
- n* now at CERN, Geneva, Switzerland
- o* also affiliated with Universtiy College London, UK
- p* now at Goldman Sachs, London, UK
- q* also at Institute of Theoretical and Experimental Physics, Moscow, Russia
- r* also at FPACS, AGH-UST, Cracow, Poland
- s* partially supported by Warsaw University, Poland
- t* supported by the Alexander von Humboldt Foundation
- u* now at Istituto Nucleare di Fisica Nazionale (INFN), Pisa, Italy
- v* now at Haase Energie Technik AG, Neumünster, Germany
- w* now at Department of Physics, University of Bonn, Germany
- x* also affiliated with DESY, Germany
- y* also at University of Tokyo, Japan
- z* now at Kobe University, Japan
- † deceased
- aa* supported by DESY, Germany
- ab* member of National Technical University of Ukraine, Kyiv Polytechnic Institute, Kyiv, Ukraine
- ac* member of National University of Kyiv - Mohyla Academy, Kyiv, Ukraine
- ad* Alexander von Humboldt Professor; also at DESY and University of Oxford
- ae* STFC Advanced Fellow
- af* now at LNF, Frascati, Italy
- ag* This material was based on work supported by the National Science Foundation, while working at the Foundation.
- ah* also at Max Planck Institute for Physics, Munich, Germany, External Scientific Member
- ai* now at Tokyo Metropolitan University, Japan

- aj* now at Nihon Institute of Medical Science, Japan
- ak* now at Osaka University, Osaka, Japan
- al* also at Łódź University, Poland
- am* member of Łódź University, Poland
- an* now at Department of Physics, Stockholm University, Stockholm, Sweden
- ao* also at Cardinal Stefan Wyszyński University, Warsaw, Poland

1 Introduction

The production of electroweak bosons in ep collisions is a good benchmark process for testing the Standard Model (SM). Even though the expected numbers of events for W^\pm and Z^0 production are low, the measurement of the cross sections of these processes is important as some extensions of the SM predict anomalous couplings and thus changes in these cross sections. A measurement of the cross section for W^\pm production at HERA has been performed by H1 and ZEUS [1] in events containing an isolated lepton and missing transverse momentum, giving a cross section $\sigma(ep \rightarrow W^\pm X) = 1.06 \pm 0.17$ (stat. \oplus syst.) pb, in good agreement with the SM prediction. The cross section for Z^0 production is predicted to be 0.4 pb.

This paper reports on a measurement of the production of Z^0 bosons in $e^\pm p$ collisions using an integrated luminosity of about 0.5 fb^{-1} . The hadronic decay mode was chosen¹ because of its large branching ratio and because it allows the excellent resolution of the ZEUS hadronic calorimeter to be exploited to the full. The analysis was restricted to elastic and quasi-elastic Z^0 production in order to suppress QCD multi-jet background. The selected process is $ep \rightarrow eZ^0 p^{(*)}$, where $p^{(*)}$ stands for a proton (elastic process) or a low-mass nucleon resonance (quasi-elastic process).

Figure 1 shows a leading-order (LO) diagram of Z^0 production with subsequent hadronic decay. In such events, there are at least two hadronic jets with high transverse energies, and no hadronic energy deposits around the forward² direction, in contrast to what would be expected in inelastic collisions.

2 Experimental set-up

HERA was the world's only high-energy ep collider, with an electron³ beam of 27.6 GeV and a proton beam of 920 GeV (820 GeV until 1997). For this analysis, $e^\pm p$ collision data collected with the ZEUS detector between 1996 and 2007, amounting to 496 pb^{-1} of integrated luminosity, have been used. They consist of 289 pb^{-1} of e^+p data and 207 pb^{-1} of e^-p data.

¹ The Z^0 decay into charged lepton pairs was studied in a previous ZEUS publication [2].

² The ZEUS coordinate system is a right-handed Cartesian system, with the Z axis pointing in the proton beam direction, referred to as the forward direction, and the X axis pointing towards the centre of HERA. The coordinate origin is at the nominal interaction point. The pseudorapidity is defined as $\eta = -\ln(\tan \frac{\theta}{2})$, where the polar angle, θ , is measured with respect to the proton beam direction.

³ The term electron also refers to positrons if not stated otherwise.

After 2003, HERA was operated with a polarised lepton beam. When combining the data taken with negative and positive polarisations, the average polarisation is less than 1% and its effect was neglected in this analysis.

A detailed description of the ZEUS detector can be found elsewhere [3]. A brief outline of the components that are most relevant for this analysis is given below.

Charged particles were tracked in the central tracking detector (CTD) [4], which operated in a magnetic field of 1.43 T provided by a thin superconducting solenoid. The CTD consisted of 72 cylindrical drift chamber layers, organised in nine superlayers covering the polar-angle region $15^\circ < \theta < 164^\circ$. For the data taken after 2001, the CTD was complemented by a silicon microvertex detector (MVD) [5], consisting of three active layers in the barrel and four disks in the forward region.

The high-resolution uranium–scintillator calorimeter (CAL) [6] consisted of three parts: the forward (FCAL), the barrel (BCAL) and the rear (RCAL) calorimeters. Each part was subdivided transversely into towers and longitudinally into one electromagnetic section (EMC) and either one (in RCAL) or two (in BCAL and FCAL) hadronic sections (HAC). The smallest subdivision of the calorimeter was called a cell. The CAL energy resolutions, as measured under test-beam conditions, were $\sigma(E)/E = 0.18/\sqrt{E}$ for electrons and $\sigma(E)/E = 0.35/\sqrt{E}$ for hadrons, with E in GeV.

The luminosity was measured using the Bethe–Heitler reaction $ep \rightarrow e\gamma p$ by a luminosity detector which consisted of independent lead–scintillator calorimeter [7] and magnetic spectrometer [8] systems. The fractional systematic uncertainty on the measured luminosity was 2%.

3 Monte Carlo simulations

Monte Carlo (MC) simulations were made to simulate the Z^0 production process. They were used to correct for instrumental effects and selection acceptance and to provide a template for the shape of the invariant-mass distribution of the Z^0 signal. The EPVEC program [9] was used to generate the signal events at the parton level. The following Z^0 production processes are considered in EPVEC:

- elastic scattering, $ep \rightarrow eZ^0p$, where the proton stays intact;
- quasi-elastic scattering, $ep \rightarrow eZ^0p^*$, where the proton is transformed into a nucleon resonance p^* ;
- deep inelastic scattering (DIS), $\gamma^*p \rightarrow Z^0X$, in the region $Q^2 > 4 \text{ GeV}^2$, where Q^2 is the virtuality of the photon exchanged between the electron and proton;

- resolved photoproduction, $\gamma p \rightarrow (q\bar{q} \rightarrow Z^0) X$, where one of the quarks is a constituent of the resolved photon and the other quark is a constituent of the proton.

In EPVEC the first two processes are calculated using form factors and structure functions fitted directly to experimental data. Note that, even if the virtuality of the exchanged photon is small, the scattered electron could receive a large momentum transfer when the Z^0 is radiated from the lepton line. In the last two processes, the proton breaks up. The DIS process is calculated in the quark–parton model using a full set of leading-order Feynman diagrams. Resolved photoproduction is parametrised using a photon structure function and is carefully matched to the DIS region. The cross section of Z^0 production is calculated to be 0.16 pb for elastic and quasi-elastic processes and 0.24 pb for DIS and resolved photoproduction. The difference between e^+p and e^-p cross sections is negligible for this analysis (1% for the DIS process). A correction, based on the MC cross section, was made to account for the part of data taken at the centre-of-mass energy $\sqrt{s} = 300$ GeV, so that the result is quoted at $\sqrt{s} = 318$ GeV.

After the parton-level generation by EPVEC, PYTHIA 5.6 [10] was used to simulate initial- and final-state parton showers with the fragmentation into hadrons using the Lund string model [11] as implemented in JETSET 7.3 [10]. The generated MC events were passed through the ZEUS detector and trigger simulation programs based on GEANT 3.13 [12]. They were reconstructed and analysed by the same programs as the data.

A reliable prediction of background events with the signal topology, which are predominantly due to the diffractive photoproduction of jets of high transverse momentum, is currently not available. Therefore, the background shape of the invariant-mass distribution was estimated with a data-driven method. The normalisation was determined by a fit to the data.

4 Event reconstruction and selection

The events used in this analysis were selected online by the ZEUS three-level trigger system [13], using a combination of several trigger chains which were mainly based on requirements of large transverse energy deposited in the calorimeter. In the offline selection, further criteria were imposed in order to separate the signal from the background.

The events are characterised by the presence of at least two jets of high transverse energy and, for a fraction of events, by the presence of a reconstructed scattered electron. In order to select events with a Z^0 decaying hadronically, jets were reconstructed in the hadronic final state using the k_T cluster algorithm [14] in the longitudinally invariant inclusive mode [15]. The algorithm was applied to the energy clusters in the CAL after excluding those associated with the scattered-electron candidate [16–18]. Energy corrections [19–21]

were applied to the jets in order to compensate for energy losses in the inactive material in front of the CAL.

In this analysis, only jets with $E_T > 4 \text{ GeV}$ and $|\eta| < 2.0$ were used. Here E_T is the jet transverse energy and η its pseudorapidity. The hadronic Z^0 decay sample was selected by the following requirements on the reconstructed jets:

- at least two jets in the event had to satisfy $E_T > 25 \text{ GeV}$;
- $|\Delta\phi_j| > 2 \text{ rad}$, where $\Delta\phi_j$ is the azimuthal difference between the first and second highest- E_T jet, as the two leading jets from the Z^0 boson decays are expected to be nearly back-to-back in the X - Y plane.

Electrons were reconstructed using an algorithm that combined information from clusters of energy deposits in the CAL and from tracks [16]. To be defined as well-reconstructed electrons, the candidates were required to satisfy the following selection:

- $E'_e > 5 \text{ GeV}$ and $E_{\text{in}} < 3 \text{ GeV}$, where E'_e is the scattered electron energy and E_{in} is the total energy in all CAL cells not associated with the cluster of the electron but lying within a cone in η and ϕ of radius $R = \sqrt{\Delta\eta^2 + \Delta\phi^2} = 0.8$, centred on the cluster;
- If the electron was in the acceptance region of the tracking system, a matched track was required with momentum $p_{\text{track}} > 3 \text{ GeV}$. After extrapolating the track to the CAL surface, its distance of closest approach (DCA) to the electron cluster had to be within 10 cm.

The following cuts were applied to suppress low- Q^2 neutral-current and direct-photoproduction backgrounds:

- $E_{\text{RCAL}} < 2 \text{ GeV}$, where E_{RCAL} is the total energy deposit in RCAL;
- $50 < E - p_Z < 64 \text{ GeV}$, where $E - p_Z = \sum_i E_i (1 - \cos \theta_i)$; E_i is the energy of the i -th CAL cell, θ_i is its polar angle and the sum runs over all cells⁴;
- $\theta_e < 80^\circ$ for well reconstructed electrons, where θ_e is the polar angle of the scattered electron, motivated by the fact that, due to the large mass of the produced system, the electron is backscattered to the forward calorimeter or forward beam pipe;
- the event was rejected if more than one electron candidate was found;
- jets were regarded as a misidentified electron or photon and were discarded from the list of jets if the direction of the jet candidate was matched within $R < 1.0$ with that of an electron candidate identified by looser criteria⁵ than those described above. This

⁴ For fully contained events, or events in which the particles escape only in the forward beam pipe, the $E - p_Z$ value peaks around twice the electron beam energy, 55 GeV.

⁵ Candidates were selected by less stringent requirements and clusters with no tracks were also accepted to find photons and electrons.

cut causes a loss of acceptance of about 3%.

To remove cosmic and beam–gas backgrounds, events fulfilling any of the conditions listed below were rejected:

- $|Z_{\text{vtx}}| > 50$ cm, where Z_{vtx} is the Z position of the primary vertex reconstructed from CTD+MVD tracks;
- $175^\circ < (\theta_{\text{jet1}} + \theta_{\text{jet2}}) < 185^\circ$ and $\Delta\phi_j > 175^\circ$ simultaneously, where θ_{jet1} and θ_{jet2} are the polar angles of the first and second highest- E_T jet, respectively, and $\Delta\phi_j$ is the azimuthal difference between them;
- $|t_u - t_d| > 6.0$ ns, where $|t_u - t_d|$ is the timing difference between the upper and the lower halves of the BCAL;
- $\cancel{p}_T > 25$ GeV, where \cancel{p}_T is the missing transverse momentum calculated from the energy clusters in the CAL;
- $N_{\text{trk}}^{\text{vtx}} < 0.25 (N_{\text{trk}}^{\text{all}} - 20)$, where $N_{\text{trk}}^{\text{vtx}}$ is the number of tracks associated with the primary vertex and $N_{\text{trk}}^{\text{all}}$ is the total number of tracks [22].

The number of events passing the above selection was 5257. Finally, to select the elastic and quasi-elastic processes preferentially, a cut on η_{max} was introduced,

- $\eta_{\text{max}} < 3.0$.

The quantity η_{max} was defined as the pseudorapidity of the energy deposit in the calorimeter closest to the proton beam direction with energy greater than 400 MeV as determined by calorimeter cells. This cut also rejected signal events which have energy deposits from the scattered electron in the calorimeter around the forward beam pipe, causing an acceptance loss of about 30%.

After all selection cuts, 54 events remained. The total selection efficiency was estimated by the MC simulation to be 22% for elastic and quasi-elastic processes and less than 1% for DIS and resolved photoproduction events. The number of expected signal events in the final sample, as predicted by EPVEC, is 18.3. The contribution from elastic and quasi-elastic processes amounts to 17.9 events.

5 Background-shape study

Figure 2a shows the distribution of the invariant mass, M_{jets} , after all the selection criteria except for the requirement $\eta_{\text{max}} < 3.0$. The variable M_{jets} was calculated using all jets passing the selection criteria described in Section 4. Figures 2b-d show M_{jets} for various η_{max} slices in the inelastic region ($\eta_{\text{max}} > 3.0$) for the same selection. No significant

dependence on η_{\max} of the M_{jets} distribution beyond that expected from statistical fluctuations was observed in the inelastic region. In addition, the shape of the M_{jets} distribution outside the Z^0 mass window in the region $\eta_{\max} < 3.0$ was found to be consistent with that in the inelastic region (Fig. 3). Therefore, the M_{jets} distribution in the inelastic region was adopted as a background template in a fit to the data in the elastic region as described in the following section.

6 Cross-section extraction

A fit to the sum of the signal and a background template for the M_{jets} distribution was used for the cross-section extraction. The template $N_{\text{ref},i}$ is defined according to:

$$N_{\text{ref},i} = aN_{\text{sg},i}^{\text{MC}}(\epsilon) + bN_{\text{bg},i}^{\text{data}}, \quad (1)$$

where i is the bin number of the M_{jets} distribution. The parameter ϵ accounts for a possible energy shift, i.e. $M_{\text{jets}} = (1 + \epsilon) M_{\text{jets}}^{\text{MC}}$, where $M_{\text{jets}}^{\text{MC}}$ is the invariant-mass distribution of the signal Z^0 MC. The quantity $N_{\text{sg},i}^{\text{MC}}$ is a signal template estimated from the Z^0 MC distribution after all cuts, normalised to data luminosity. The quantity $N_{\text{bg},i}^{\text{data}}$ is a background template determined from the data outside the selected region. The parameters a and b are the normalisation factors for the signal and background, respectively. The likelihood of the fit, \mathcal{L} , is defined as follows:

$$\mathcal{L} = \mathcal{L}_1(N_{\text{obs}}, N_{\text{ref}}) \times \mathcal{L}_2(\epsilon, \sigma_\epsilon), \quad (2)$$

with

$$\mathcal{L}_1 = \prod_i \frac{\exp(-N_{\text{ref},i}) (N_{\text{ref},i})^{N_{\text{obs},i}}}{N_{\text{obs},i}!} \quad \text{and} \quad \mathcal{L}_2 = \exp\left(-\frac{\epsilon^2}{2\sigma_\epsilon^2}\right).$$

Here $\mathcal{L}_1(N_{\text{obs}}, N_{\text{ref}})$ is the product of Poisson probabilities to observe $N_{\text{obs},i}$ events for the bin i when $N_{\text{ref},i}$ is expected. The term $\mathcal{L}_2(\epsilon, \sigma_\epsilon)$ represents the Gaussian probability density for a shift ϵ of the jet energy scale from the nominal scale, which has a known systematic uncertainty of $\sigma_\epsilon = 3\%$. From the likelihood, a chi-squared function is defined as

$$\tilde{\chi}^2 = -2 \ln \frac{\mathcal{L}_1(N_{\text{obs}}, N_{\text{ref}})}{\mathcal{L}_1(N_{\text{obs}}, N_{\text{obs}})} - 2 \ln \mathcal{L}_2 = 2 \sum f_i + \left(\frac{\epsilon}{\sigma_\epsilon}\right)^2, \quad (3)$$

with

$$f_i = \begin{cases} N_{\text{ref},i} - N_{\text{obs},i} + N_{\text{obs},i} \ln(N_{\text{obs},i}/N_{\text{ref},i}) & (\text{if } N_{\text{obs},i} > 0) \\ N_{\text{ref},i} & (\text{if } N_{\text{obs},i} = 0). \end{cases}$$

The best combination of (a, b, ϵ) is found by minimising $\tilde{\chi}^2$. The value of a after this optimisation gives the ratio between the observed and expected cross section, i.e. $\sigma_{\text{obs}} = a\sigma_{\text{SM}}$. The maximum and minimum values of a in the interval $\Delta\tilde{\chi}^2 < 1$ define the range of statistical uncertainty.

7 Systematic uncertainties

Several sources of systematic uncertainties were considered and their impact on the measurement estimated.

- An uncertainty of 3% was assigned to the energy scale of the jets and the effect on the acceptance correction was estimated using the signal MC. The uncertainty on the Z^0 cross-section measurement was estimated to be +2.1% and -1.7%.
- The uncertainty associated with the elastic and quasi-elastic selection was considered. In a control sample of diffractive DIS candidate events, the η_{\max} distribution of the MC agreed with the data to within a shift of η_{\max} of 0.2 units [23]. Thus, the η_{\max} threshold was changed in the signal MC by ± 0.2 , and variations of the acceptance were calculated accordingly. The uncertainty on the cross-section measurement was +6.4% and -5.4%.
- The background shape uncertainty was estimated by using different slices of η_{\max} in the fit. The background shape was obtained using only the regions of $4.0 < \eta_{\max} < 4.2$ or $4.2 < \eta_{\max}$. The region of $3.0 < \eta_{\max} < 4.0$ was not used since a small number of signal events is expected in this η_{\max} region⁶. The resulting uncertainty in the cross-section measurement was $\pm 1.5\%$.
- The uncertainty associated with the luminosity measurement was estimated to be 2%, as described in Section 2.
- The Z^0 mass distribution from the MC used as a signal template has a Gaussian core width of 6 GeV. A possible systematic uncertainty coming from the width of the MC signal peak was studied. The mass fit was repeated after smearing the Z^0 mass distribution in the MC by a Gaussian function with different widths. The measured cross section did not change significantly after smearing the distribution up to the point where the fit $\tilde{\chi}^2$ changed by 1. No systematic uncertainty from this source was assigned.

The total systematic uncertainty was calculated by summing the individual uncertainties in quadrature and amounts to +7.2% and -6.2%.

8 Results and conclusions

Figure 3 shows the invariant-mass distribution of the selected events. It also shows the fit result for the signal plus background and the background separately. The fit yielded a

⁶ The ratio of the expected number of signal MC events to the observed data in this region was estimated to be 2.6% for $80 < M_{\text{jets}} < 100$ GeV, while in the other slices it was less than 0.4%.

result for the parameter a from Eq. 1 of $a = 0.82_{-0.35}^{+0.38}$. That translates into a number of observed Z^0 events of $15.0_{-6.4}^{+7.0}$ (stat.), which corresponds to a signal with a 2.3σ statistical significance. The fit yielded a value for the energy shift ϵ of $0.028_{-0.020}^{+0.021}$, which is compatible with zero. The quality was evaluated according to Eq. 3; the value of $\tilde{\chi}^2/ndf = 17.6/22$, where ndf is the number of degrees of freedom, indicates a good fit. The cross section for the elastic and quasi-elastic production of Z^0 bosons, $ep \rightarrow eZ^0p^{(*)}$, at $\sqrt{s} = 318$ GeV, was calculated to be

$$\sigma(ep \rightarrow eZ^0p^{(*)}) = 0.13 \pm 0.06 \text{ (stat.)} \pm 0.01 \text{ (syst.) pb.} \quad (4)$$

This result is consistent with the SM cross section calculated with EPVEC of 0.16 pb. This represents the first observation of Z^0 production in ep collisions.

Acknowledgements

We appreciate the contributions to the construction and maintenance of the ZEUS detector of many people who are not listed as authors. The HERA machine group and the DESY computing staff are especially acknowledged for their success in providing excellent operation of the collider and the data-analysis environment. We thank the DESY directorate for their strong support and encouragement.

References

- [1] H1 and ZEUS Coll., F.D. Aaron et al., JHEP **03**, 035 (2010).
- [2] S. Chekanov et.al., Phys. Lett. **680**, 13 (2009).
- [3] ZEUS Coll., U. Holm (ed.), *The ZEUS Detector*. Status Report (unpublished), DESY (1993), available on <http://www-zeus.desy.de/bluebook/bluebook.html>.
- [4] N. Harnew et al., Nucl. Inst. Meth. **A 279**, 290 (1989);
B. Foster et al., Nucl. Phys. Proc. Suppl. **B 32**, 181 (1993);
B. Foster et al., Nucl. Inst. Meth. **A 338**, 254 (1994).
- [5] A. Polini et al., Nucl. Inst. Meth. **A 581**, 656 (2007).
- [6] M. Derrick et al., Nucl. Inst. Meth. **A 309**, 77 (1991);
A. Andresen et al., Nucl. Inst. Meth. **A 309**, 101 (1991);
A. Caldwell et al., Nucl. Inst. Meth. **A 321**, 356 (1992);
A. Bernstein et al., Nucl. Inst. Meth. **A 336**, 23 (1993).
- [7] J. Andruszków et al., Preprint DESY-92-066, DESY, 1992;
ZEUS Coll., M. Derrick et al., Z. Phys. **C 63**, 391 (1994);
J. Andruszków et al., Acta Phys. Pol. **B 32**, 2025 (2001).
- [8] M. Helbich et al., Nucl. Inst. Meth. **A 565**, 572 (2006).
- [9] U. Baur, J.A.M. Vermaseren and D. Zeppenfeld, Nucl. Phys. **B 375**, 3 (1992).
- [10] T. Sjöstrand, PYTHIA 5.6 and JETSET 7.3 *Physics and Manual*, 1992.
CERN-TH.6488/92.
- [11] B. Andersson et al., Phys. Rep. **97**, 31 (1983).
- [12] R. Brun et al., GEANT3, Technical Report CERN-DD/EE/84-1, CERN, 1987.
- [13] W.H. Smith, K.Tokushuku and L.W. Wiggers, *Proc. Computing in High-Energy Physics (CHEP), Annecy, France, Sept. 1992*, C. Verkerk and W. Wojcik (eds.), p. 222. CERN, Geneva, Switzerland (1992). Also in preprint DESY 92-150B.
- [14] S. Catani et al., Nucl. Phys. **B 406**, 187 (1993).
- [15] S.D. Ellis and D.E. Soper, Phys. Rev. **D 48**, 3160 (1993).
- [16] ZEUS Coll., J. Breitweg et al., Eur. Phys. J. **C 11**, 427 (1999).
- [17] G.M. Briskin. Ph.D. Thesis, Tel Aviv University, Report DESY-THESIS 1998-036, 1998, available on
<http://www-library.desy.de/preparch/desy/thesis/desy-thesis-98-036.pdf>.
- [18] L.L. Wai, Preprint UMI-96-06968, 1995.

- [19] ZEUS Coll., S. Chekanov et al., Phys. Lett. **B 547**, 164 (2002).
- [20] ZEUS Coll., S. Chekanov et al., Phys. Lett. **B 558**, 41 (2003).
- [21] ZEUS Coll., S. Chekanov et al., Phys. Lett. **B 531**, 9 (2002).
- [22] ZEUS Coll., S. Chekanov et al., Phys. Lett. **B 539**, 197 (2002). Erratum in Phys. Lett. **B 552**, 308 (2003).
- [23] V. Sola. Ph.D. Thesis, Turin University, Report DESY-THESIS-2012-008, 2012, available on <http://www-library.desy.de/preparch/desy/thesis/desy-thesis-12-008.pdf>.

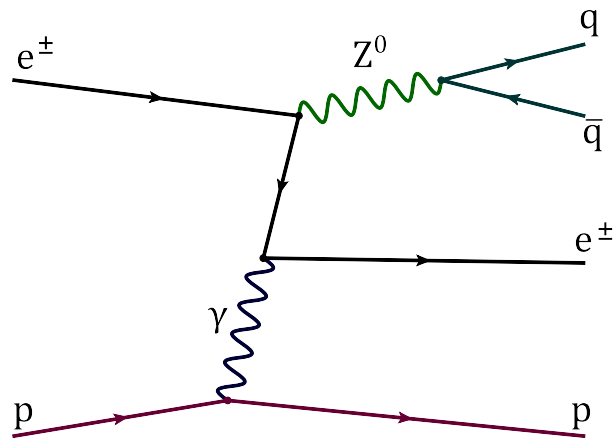


Figure 1: Example of a leading-order diagram of Z^0 boson production and subsequent hadronic decay (into quark q and antiquark \bar{q}) in $ep \rightarrow eZ^0p$.

ZEUS

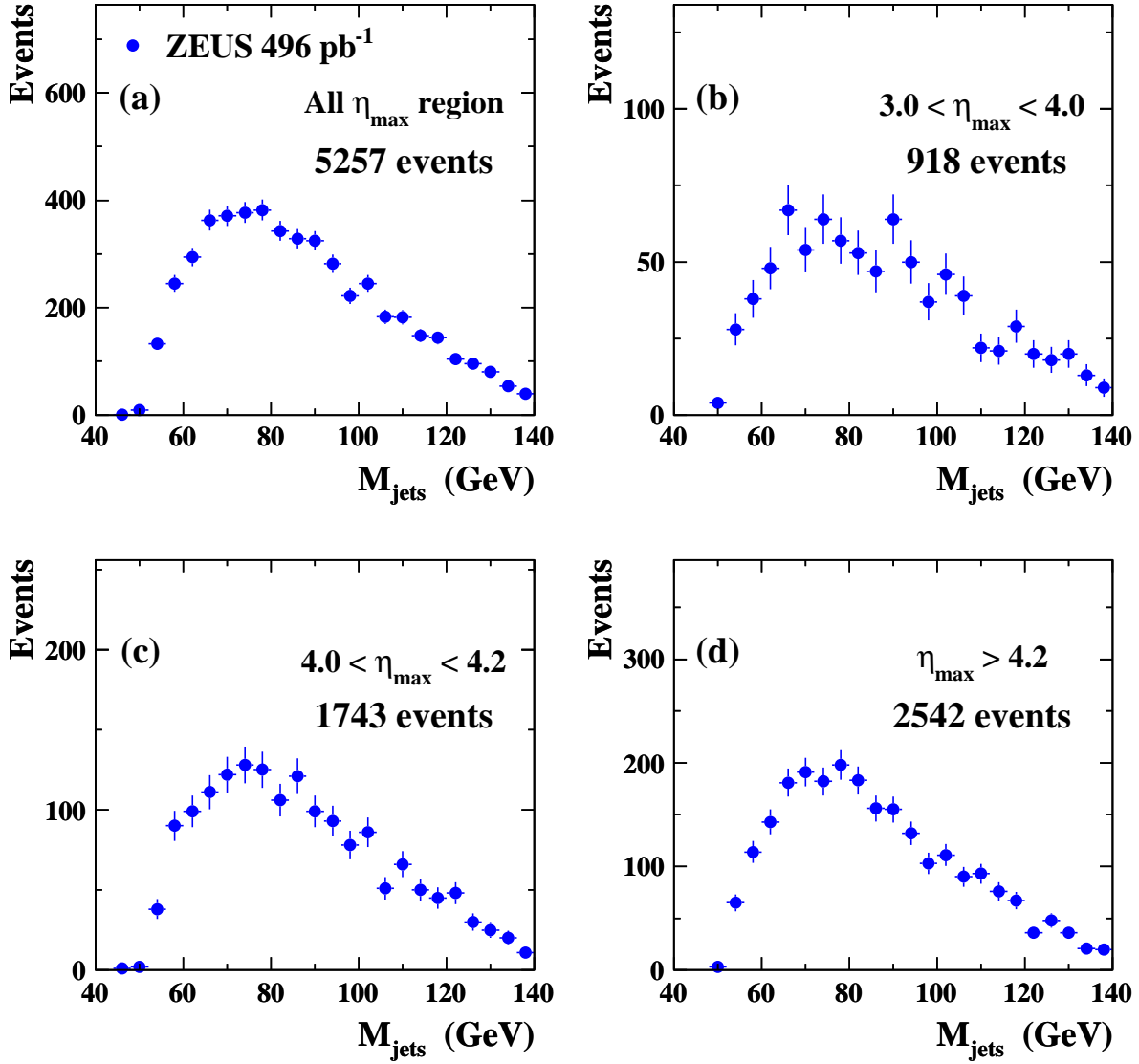


Figure 2: The M_{jets} distribution of the data (a) after all selection criteria, except for the η_{max} cut, (b-d) in several η_{max} slices.

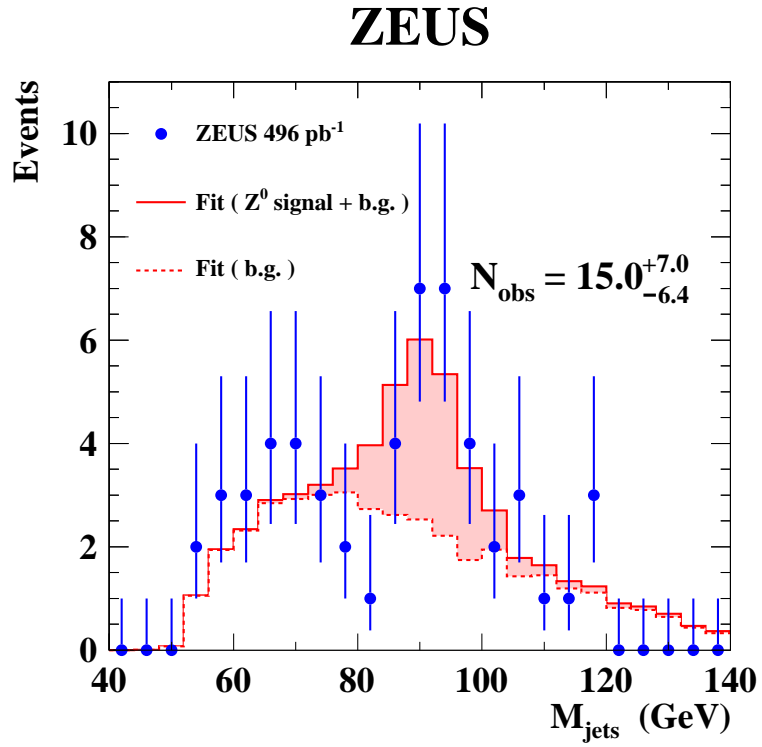


Figure 3: The M_{jets} distribution and the fit result. The data are shown as points, and the fitting result of signal+background(background component) is shown as solid (dashed) line. The signal contribution is also indicated by the shaded area and amounts to a total number of N_{obs} events. The error bars represent the approximate Poissonian 68% CL intervals, calculated as $\pm\sqrt{n + 0.25} + 0.5$ for a given entry n .